A Supercapacitor Based on Graphite Paper

By

Enchong Liu, B.Eng.

A Thesis

Submitted to the School of Graduate Studies

in Partial Fulfilment of Requirements

for the Degree

Master of Applied Science

MASTER OF APPLIED SCIENCE (2021)
McMaster University, Hamilton, Ontario
Faculty of Material Science and Engineering, Engineering Graduate Program

TITLE:	A Supercapacitor Based on Graphite Paper
AUTHOR:	Enchong Liu, B.Eng. (University of Science and Technology Beijing)
SUPERVISOR:	Dr. Gu Xu
COMMITTEE MEMBERS:	Dr. Joey Kish Dr. Igor Zhitomirsky
NUMBER OF PAGES:	72

ACKNOWLEDGMENTS

I owe a debt of thanks to Dr. Gu Xu, whose careful and able research was of great help. In the process of guiding students, he showed countless patience. When I was most helpless and chose to close myself, He didn't blame me and gave me full understanding. Thank you for your kindness and let me through the most difficult time.

Secondly, I must thank my best friend, Zhiling Luo, Associate professor at Fujian Normal University, China. He helped me at all costs when I was most desperate. In this research, he provided a lot of experimental tools and testing instruments. He spared no effort to help solve all kinds of unexpected problems encountered during the experiment. Without his help, I couldn't finish my work on time. He is not only a friend, but also a good teacher.

Thirdly, my colleagues in Xu's Research Group also helped me a lot. Hereby I must express my great gratitude to Ryan T. Wang, Lory W. Yang and Alex F. Xu for their assistance in the research. Also, thank Kelvin J. Xu for providing Basic framework of simulation.

I appreciate my committee members for their time and patience. I want to give my appreciation to all the professors, the technicians, and staff, whose work is brilliant and of great help.

Finally, I must give my deepest thanks to my parents and sister. It was them who give me endless support, mentally and physically. It was them who always stand

by me and trust me. Thank you for countless love in the past more than twenty years. It is what I cherish in all my life.

Table of contents

List of Figures

List of Tables

List of Abbreviations

SC	supercapacitor
aSC	asymmetric supercapacitor
sSC	symmetric supercapacitor
GP	graphite paper
PANI	polyaniline
PVA	polyvinyl alcohol
APS	ammonium persulfate
ANI	aniline

Abstract

As a new energy storage device, supercapacitor (SC) has attracted much attention because of its advantages like long service life, high power, and environmental protection. In the study of SCs, Polyaniline (PANI) has attracted great attention because of its high conductivity and good stability. But the working voltage of PANI based electrode is low (≤0.8V) as it usually gets crushed under higher voltage. Therefore, slowing down the crushing of PANI and increasing the working voltage of PANI based SC has been urged for the performance improvement of this kind of SC. Despite many previous attempts, the performance has not been significantly improved. In this research, the performance has been effectively improved by introducing MnO_2 and quasi-solid electrolyte into electrode system, where Scanning electron microscopy (SEM), X-ray diffraction (XRD), X-ray photoelectron spectroscopy (XPS) and battery test system have been conducted. The specific capacitance was increased by 30% in 1000 cycle times and the working voltage was doubled. Meanwhile, the lead-in of graphite paper (GP) and quasi-solid electrolyte make SC flexible and thinner, which improve the wearability of devices.

1 Introduction

1.1 Supercapacitor

Two conductors close to each other are sandwiched with a layer of non-conductive insulating medium, which constitutes a capacitor. When a voltage is applied between the two plates of a capacitor, the capacitor will store charge. The capacitance of a device is defined as the ratio of the charge carried by the conductor to the voltage between the conductors.

In 1957, Becker first proposed the concept of supercapacitor in the patent (Simon and Gogotsi, 2008).He infiltrated porous activated carbon electrode material into electrolyte to prepare supercapacitors. Based on the principle of electric double layer capacitance, a huge capacitance was formed. In the middle and late 1990s, the concept of redox pseudocapacitance was also proposed. Compared with traditional capacitors, supercapacitor introduces electrolyte into the device structure, resulting in an electrode electrolyte interface(Gibney, 2015; Kenry et al., 2016; Kim et al., 2019; Yu et al., 2019).

Supercapacitor is a new energy storage device between traditional capacitor and rechargeable battery. It not only has the characteristics of rapid charge and discharge, but also has the energy storage characteristics of battery(Hu et al., 2015; Hou et al., 2019)

.

1.1.1 Principle of supercapacitor

According to different energy storage mechanisms, supercapacitors can be divided into electric double-layer supercapacitors and pseudocapacitor supercapacitor(Conway, 2008) , as shown in **Figure.1**.

The electric double-layer capacitor mainly generates storage energy by adsorption of pure electrostatic charge on the electrode surface. pseudocapacitor capacitor mainly realize energy storage and conversion through reversible redox reaction on and near the active electrode materials.

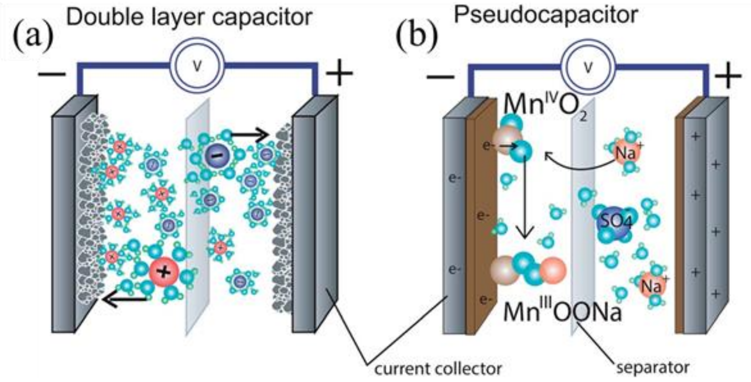

Figure. 1 Comparison of energy storage mechanisms between electric double-layer supercapacitor and pseudocapacitor supercapacitor. (a) Electric double layer supercapacitor; (b) Pseudocapacitor supercapacitor. (Jost et al., 2014)

(1) Electric double-layer capacitance (EDLC)

The electric double layer effect is formed by the separation of positive and negative charges at the electrode-electrolyte interface. It is the main mechanism of energy storage of carbon supercapacitors such as activated carbon, carbon fiber and carbon felt(Zhang and Zhao, 2009).

When charging, the potentials of the two electrodes rise and fall respectively, and a certain potential difference will be generated in the whole capacitor. Due to the different electrochemical potentials between the electrode and the electrolyte, the electrostatic charge in the electrode will attract the opposite ions in the electrolyte to the electrode surface. The potential barrier on the electrode interface ensures that the two layers of charges cannot cross the interface and neutralize each other. Therefore, a stable micro capacitance is formed at the electrode/electrolyte interface.

During discharge, the electrons on the electrode form a current through the external circuit to complete the migration, and the ions at the interface desorb back to the electrolyte.

The electric bilayer theory was first proposed by Helmholtz, as shown in **Figure.2** (a). Subsequently, this theory was further developed by Gouy – Chapman and Stern and evolved into Gouy-Chapman model (**Figure.2** (b)) and Stern model (**Figure.2** (c)). These models mainly focus on the microscopic description of the electrode electrolyte interface. For the local micro area at the interface, it is considered that it’s still ideal parallel plate capacitor. Compared with traditional electrostatic capacitors, the improvement of capacitance of electric double-layer capacitors mainly comes from the huge micro surface area of electrodes and small local electric double-layer spacing(Zhang and Zhao, 2009).

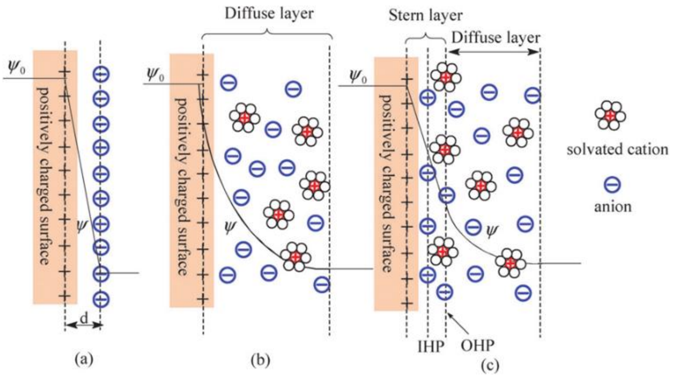

Figure. 2 Micro model of electric double layer theory. (a) Helmholtz model; (b) Gouy Chapman model; (c) Stern model, IHP and OHP in the figure are abbreviations of inner Helmholtz plate and outer Helmholtz plate respectively(Zhang and Zhao, 2009).

(2) Redox pseudo-capacitance

The energy storage mechanism of pseudocapacitor is the rapid and reversible redox reaction on the electrode surface.

When charging, electroactive substances undergo under-potential deposition and highly reversible chemical adsorption, desorption, or oxidation on the two-dimensional or quasi two-dimensional space of the electrode surface or bulk phase.

The redox pseudocapacitance is 10-100 times higher than the electric double layer capacitance. But because the redox process involves electron transfer, the power density and cycle stability of pseudocapacitor are not as good as electric double-layer supercapacitor.

Common pseudocapacitor electrode materials include transition metal oxides (such as ruthenium oxide, manganese dioxide, vanadium oxide and iron oxide), conductive polymers (such as polyaniline, polythiophene and polypyrrole) and some carbon materials containing functional groups. (Simon and Gogotsi, 2009; Jost et al., 2014; Zhang and Zhao, 2009)

In recent years, nano preparation technology is rising. Conductive polymers and transition metal oxides are prepared into nanofibers or nanoparticles to increase the specific surface area of electrode active materials to make the electrolyte fully contact with the electrode. It has both electric double-layer capacitance and redox pseudocapacitance(Pan et al., 2010)

1.1.2 Structure of supercapacitor

Supercapacitor is composed of porous electrode material with high specific surface area, fluid collector, porous battery diaphragm and electrolyte. The electrode material and the current collector shall be closely connected to reduce the contact resistance; The diaphragm shall meet the conditions of as high ionic conductivity and as low electronic conductivity as possible. It is generally an electronic insulating material with fiber structure, such as polypropylene film. The type of electrolyte is selected according to the properties of electrode materials.

1.1.3 Characterization of supercapacitors

In practical use, multiple supercapacitors need to be combined. When multiple supercapacitors C_i are connected in series, the total capacitance C_t of the device is:

$$\frac{1}{C_t}=\sum\frac{1}{C_i} \qquad (1)$$

In parallel:

$$C_t=\sum C_i \qquad (2)$$

The energy E stored after charging the supercapacitor is:

$$E = CV^2/2 \qquad (3)$$

Where V is the charging voltage. According to the discharge time t of the supercapacitor, the power P of the device can be calculated as,

$$P = E/t \qquad (4)$$

The circuit structure of the supercapacitor can be simplified to the equivalent circuit shown in **Figure. 3**. The whole device is equivalent to the series connection of the positive capacitance C_a, the negative capacitance C_c and the internal resistance R_i.

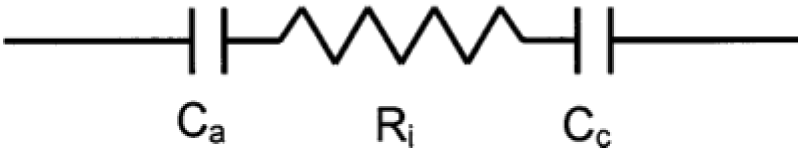

Figure. 3 Equivalent circuit of supercapacitor (Winter and Brodd, 2004)

1.1.3.1 Micro morphology characterization of electrode materials

The micro morphological characteristics of samples are characterized by scanning electron microscope and transmission electron microscope.

(1) Scanning electron microscopy (SEM)

The electron beam is scanned on the sample surface, the generated secondary electrons are collected by the detector, and the formed electrical signal is displayed on the fluorescent screen. The microstructure and morphology of the sample can be obtained clearly and intuitively by scanning electron microscope images.

(2) Transmission electron microscopy (TEM)

The electron beam emitted by the electron gun passes through the condenser along the optical axis of the mirror body in the vacuum channel, converges into a sharp, bright, and uniform light spot through the condenser, and irradiates on the sample in the sample room; The electron beam after passing through the sample carries the structural information inside the sample. The amount of electrons passing through the dense part of the sample is less, and the amount of electrons passing through the sparse part is more; After the focusing and primary amplification of the objective lens, the electron beam enters the lower intermediate lens and the first and second projection mirrors for comprehensive amplification and imaging, and finally the amplified electronic image is projected on the fluorescent screen plate in the observation room; The fluorescent screen converts the electronic image into a visible image for users to observe.

1.1.3.2 Characterization of electrochemical properties of electrode materials

The electrochemical characterization of supercapacitors mainly includes cyclic voltammetry (CV) and galvanostatic charge discharge (GCD).

(1) Cyclic voltammetry (CV)

Cyclic voltammetry is a common electrochemical research method. In this method, the electrode potential is controlled to scan repeatedly at different rates with triangular waveform for one or more times over time. The potential range enables different reduction and oxidation reactions to occur alternately on the electrode, and the current potential curve is recorded. According to the curve shape, the reversibility of electrode reaction, the possibility of intermediate, phase boundary adsorption or new phase formation, and the properties of coupling chemical reaction can be judged. It is often used to measure electrode reaction parameters, judge its control steps and reaction mechanism, and observe what reactions can occur and their properties in the whole potential scanning range.

For ideal parallel plate capacitors, capacitance is independent of voltage,

$$i = \frac{\mathrm{d}Q}{\mathrm{d}t} = \frac{C\mathrm{d}U}{\mathrm{d}t} = Cv \tag{5}$$

Equation (5) shows that for an ideal parallel plate capacitor, the cyclic voltammetry curve is a rectangle. The cyclic voltammetry curve of the actual supercapacitor deviates slightly from the rectangle because there is an equivalent resistance. When the electrode has redox reaction, there will be redox peak on the cyclic voltammetry curve. The capacitance of the device can be calculated by cyclic voltammetry curve,

$$C = \frac{1}{\Delta V}\int_{V_s}^{V_e} i\mathrm{d}t \tag{6}$$

Where ΔV is the voltage range when the supercapacitor is discharged, and V_s and V_e are the voltage starting point and voltage ending point of the device discharge process respectively.

When considering the equivalent internal resistance, the output current can change to a stable current only after a certain relaxation time. In the volt ampere cycle test curve, there is an arc curve at the potential flyback. When RC is smaller, the relaxation time is faster and the curve is closer to rectangle; When

RC is large, the relaxation time is slow and the curve deviates from the rectangle. The supercapacitance behavior and equivalent internal resistance of the device in the working voltage range can be preliminarily understood by the shape of volt ampere cycle test curve.

(2) Galvanostatic charge-discharge（GCD)

Galvanostatic charge discharge method is one of the most important methods to study the electrochemical properties of materials. Its basic working principle is: charge and discharge the measured electrode under constant current condition, record the variation law of its potential with time, then study the charge and discharge performance of the electrode and calculate its actual specific capacity. In the charge discharge experiment under constant current condition, the electrochemical response signal of the control current is applied. When the control signal of the current is applied, the potential is the measured response signal. The change law of the potential as a function of time is mainly studied.

The capacitance, equivalent internal resistance and magnification performance of the device can be obtained by constant current charge discharge test. When the current is constant, the change rate of voltage can be obtained according to equation (5),

$$\frac{\mathrm{d}U}{\mathrm{d}t}=\frac{i}{C} \tag{7}$$

That is, the change speed of voltage is inversely proportional to the capacitance, from which the capacitance of the device can be calculated. The voltage variation of some supercapacitors with time is not an ideal straight line. At this time, the curve can be linearly fitted to finally calculate the capacitance.

When the device changes from charging state to discharging state, the voltage change at both ends of the device is discontinuous, and there is an obvious jump. Based on this, the equivalent internal resistance R_i of supercapacitor can be estimated,

$$R_{\mathrm{i}}=\frac{U_1\text{-}U_2}{2i} \tag{8}$$

U_1 - U_2 is the jump of voltage, and i is the discharge current. In the actual test process, R_i is not a fixed value. The greater the discharge current, the greater the measured equivalent internal resistance, which may be related to the existence of certain polarization of the electrode(Sun et al., 2018).

The coulomb efficiency η of a supercapacitor is defined as the ratio of the charge Q_D released by the device during discharge to the charge Q_C flowing during charging, i.e

$$\eta=\frac{Q_D}{Q_{\mathrm{C}}}\times 100\%=\frac{it_D}{it_C}\times 100\% = \frac{t_D}{t_C}\times 100\% \tag{9}$$

T_C and T_D are charging and discharging time respectively. The changes of capacitance and coulomb efficiency with the number of cycles can be obtained by repeated constant current charge and discharge to characterize the cycle stability of the device.

(3) Cycle life performance

The cycle life of electrode material can be obtained by continuous and repeated constant current charge and discharge of the device. Generally, the relationship curve between specific capacitance and cycle times is obtained through this test to analyse the stability of the device.

1.2 Graphite paper

Graphite paper is made of high carbon steel phosphorus graphite by organic chemical treatment, high temperature expansion and cold rolling. It has a large specific surface area, which is conducive to the physical and chemical adsorption of polyaniline on its surface.

As a carbon material with low price, high conductivity and stable chemical properties, graphite paper is widely used to prepare the electrode of supercapacitor. The application of graphite paper in the field of capacitor preparation has more advantages than traditional materials.

1.3 Conductive polymer and polyaniline (PANI)

1.3.1 Conductive polymer

In the 1970s, MacDiarmid, Heeger and Shirakawa found that changed the room temperature conductivity of polyacetylene containing alternating single and double bonds changed from insulator (10^9S/cm) to conductor (10^3S/cm) after iodine doping, and the conductivity increased by 12 orders of magnitude (Shirakawa et al., 1977; Nigrey et al., 1979). The discovery breaks the traditional idea that organic polymers are irrelevant to conductivity.

Conductive polymer material is a polymer material with conjugate main electron system in the main chain, which can achieve conductive state through doping, and the conductivity is more than 1000S/cm.

Conductive polymers can be divided into two categories:

(1) Composite type, that is, it is composed of polymer as matrix and conductive components such as starch or fibrous metal and graphite. It can be prepared into conductive products such as plastics, rubber, coatings, and adhesives. This kind has been widely used.

(2) Structural type, that is, polymers with special structure have conductivity. This kind of polymer is an international frontier research topic, and some of them are in the process of application.

The doping of conductive polymers is different from that of inorganic semiconductors: the doping of inorganic semiconductors is to replace atoms, such as adding a small amount of second substances with different valence states to high-purity silicon, germanium or gallium, so as to change the original distribution state of electrons and holes in the material, The amount of this doping is very low (a few ten thousandths), and once doped, it cannot be de doped; the doping of conductive polymers is a redox process, which is essentially charge transfer. The amount of this doping is huge (up to 50%), not only the doping process, but also the de doping process, and the two are completely reversible(Eftekhari and Jafarkhani, 2014; Bian et al., 2012; Tangury et al., 2018)

1.3.2 polyaniline (PANI)

Typical representatives of conductive polymers include polyacetylene, polyaniline, polypyrrole, polythiophene and their derivatives. Although polyacetylene is the representative of conductive polymers, its practical application is seriously limited due to its poor environmental stability. With the in-depth development of conductive polymer research, polyaniline, polypyrrole and polythiophene have become three major varieties of concern. Polyaniline has attracted great attention because of its high conductivity after doping, good stability in room temperature air, simple preparation method and controllable conditions(Rudge et al., 1994; Arbizzani et al., 1996; Mastragostino et al., 1996; Hu and Chu, 2001).

1.3.2.1 Structure of polyaniline

In 1987, MacDiarmid proposed a more reasonable polyaniline polymer chain structure, as shown in **Figure. 4**.

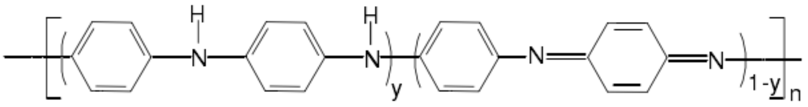

（$0 \leq y \leq 1$）

Figure. 4 Polymer structure of Polyaniline(Macdiarmid et al., 1987)

y value represents the redox degree of polyaniline, and polyaniline with different oxidation degree shows different composition, structure, color, and conductivity characteristics. When y=0, it is a "benzene-quinone" alternating oxidation state structure (Pernigraniline, PNB); when y=1, it is a fully reduced "benzene-benzene" structure (Leucoemeraldine, LEB); when 0<y<1, it is an intermediate oxidation state, especially when y=0.5, it is a semi oxidation and semi reduction state (Emeraldine, EB) with a benzene/quinone ratio of 3:1.

When y=0.5, the structure is the most favorable structure for carrier transport after doping. When y=0 or y=1, both the intrinsic state and the doped state are electrically insulating.

During the transformation from completely reduced state (Leucoemeraldiline, LB, y=1) to completely oxidized state (Pernigraniline, PNB, y = 0), polyaniline showed yellow, green, dark blue, dark purple and black with the increase of oxidation degree.

1.3.2.2 Properties of polyaniline

(1) Conductivity

The conductivity of polyaniline depends on the degree of oxidation and doping of the polymer.

When pH < 4, polyaniline is an insulator, and the conductivity is independent of pH; When 4 > pH > 2, the conductivity increases rapidly with the increase of pH, which is directly due to the increase of doping degree; When pH < 2, the conductivity is independent of pH, and the polymer is metallic.

When the conductivity and temperature are in a certain temperature range, it can be considered that the conductivity increases with the increase of temperature. At a certain pH value, the conductivity increases gradually with the increase of potential, and then reaches a platform. However, when the potential continues to rise, the conductivity decreases sharply, and finally presents the behavior of insulator. The change of scanning potential is reflected in the structure of polyaniline, indicating that in the state of polyaniline, the highest oxidation state and the lowest reduction state are insulated, while only the middle semi oxidation state is conductive(Wu et al., 2005; Gawli et al., 2016; Patil et al., 2011; Giri et al., 2013; Zhang et al., 2011).

(2) Solubility

Due to the strong rigidity of polyaniline chain and strong interaction between chains. Its solubility is very poor, and the processability is also very poor(Fan et al., 2007).

The study of polyaniline with good solubility based on high conductivity has become a concern. Since 1992, scholars first synthesized chlorinated polystyrene (PSSA) polyaniline with water soluble PSSA as the reaction template and high-speed rail as oxidant. Many scholars used water/oil two-phase emulsion polymerization to prepare soluble polyaniline with DBSA as emulsifier and dopant and thiosulfate as initiator(Cho et al., 2013; Chen et al., 2013; Zhou et al., 2018).

1.3.2.3 Synthesis of polyaniline

The main synthetic methods of polyaniline are chemical oxidation method and electrochemical method(Zhang and Wang, 2006).

(1) Chemical oxidation method

The chemical oxidative polymerization of polyaniline is the oxidative polymerization of aniline monomer with oxidant in acidic aqueous solution. Large quantities of polyaniline can be prepared by chemical oxidation, which is also the most used method to prepare polyaniline.

The synthesis of polyaniline by chemical oxidation is mainly affected by the type and concentration of reaction medium acid, the type and concentration of oxidant, monomer concentration, reaction temperature and reaction time. Protonic acid is an important factor affecting the oxidative polymerization of aniline. It mainly plays two roles: providing the pH value required by the reaction medium and entering the polyaniline skeleton in the form of dopant to give it a certain conductivity.

The initiators used mainly include $(NH_4)_2S_2O_8$(Ma et al., 2009), $K_2Cr_2O_7$(Ayad et al., 2004), KIO_3(Hirase et al., 2014), $FeCl_3$(Gosk et al., 2016), H_2O_2(Sarma et al., 2002), Ce $(SO_4)_2$(Elkais et al., 2011), MnO_2(Mezgebe et al., 2019) and BPO (benzoyl peroxide) (Ram and Palaniappan, 2003). The properties of polyaniline obtained are basically the same. Among them, $(NH_4)_2S_2O_8$ is the most widely used oxidant because it does not contain metal ions, has strong oxidation capacity and convenient post-treatment.

(2) Electrochemical method

Electrochemical preparation of polyaniline is to select appropriate electrochemical conditions in the electrolyte solution containing aniline to make the oxidation polymerization of aniline on the anode to produce polyaniline film adhered to the electrode surface or polyaniline powder deposited on the electrode surface(Xie et al., 2016; Pham-Cong et al., 2017; Alguail et al., 2016).

Electrochemical methods include cyclic voltammetry, galvanostatic method, potentiostatic method, etc. Among them, the polyaniline film prepared by cyclic voltammetry has uniform texture, good conductivity, excellent redox reversibility and can obtain self-supporting film, which is of great significance to study the polymerization mechanism of polyaniline, doping organic matter and electrode modification(Vega-Rios et al., 2013; Jayakumar et al., 2015; Yu el al., 2016; Wang et al., 2016; Miao et al., 2016).

Polyaniline synthesized by electrochemical method has high purity, simple reaction conditions and easy control. However, electrochemical method is only suitable for the synthesis of small quantities of polyaniline(Imani et al., 2015; Uppugalla et al., 2014; Dhibar et al., 2014; Xiang et al., 2016).

1.3.2.4 Application of polyaniline

Polyaniline has potential application value in many aspects.

In the case of supercapacitors, polyaniline is an excellent pseudocapacitor electrode material. Based on the reversible process of oxidation-reduction, polyaniline can convert from reduced state to intermediate oxidation state to highest oxidation state.

In addition, polyaniline can be used for Anticorrosive coating(Lu et al., 1995), selective electrode(Zhou et al., 2018), Antistatic and electromagnetic shielding materials(Bhandari et al., 2009), Special separation membrane(Sairam et al., 2006), electrochromic device(Kobayashi et al., 1984), organic light emitting diodes(Burroughes et al., 1990).

1.4 MnO_2

Electrode materials used in supercapacitors mainly include carbon materials(He et al., 2014; Li et al., 2017; Güven Özdemir et al., 2015), conductive polymers(Sun et al., 2015; Bahloul et al., 2013) and transition metal oxides(Wang et al., 2016; Yang et al., 2015; Yu et al., 2016). In transition metal oxides, the potential window of Co_3O_4 and NiO is relatively narrow(Liu et al., 1996; Lin et al., 1998) and RuO_2 is expensive. MnO_2 with low price and high potential window has attracted the attention of researchers.

1.4.1 Storage mechanisms of MnO_2

Most of the capacitance produced by MnO_2 as electrode material is pseudocapacitance. In the process of charge and discharge, the electricity is stored by rapid and reversible redox reaction between Mn (III) and Mn (IV).

The energy storage mechanism of MnO_2 as capacitor electrode material is very complex. Kozawa's proton-electron theory has been widely recognized(Kozawa and Powers, 1969). The reaction can be separated into two steps:

(1) Primary reaction:

MnO_2 is reduced to MnOOH. In this process, the protons in the electrolyte directly pass through the electric double layer on the solid-liquid interface of MnO_2 particles to the surface of MnO_2 lattice and combine with O^{2-} to form OH^-, Mn^{4+} is reduced to Mn^{3+}.The reaction formula is:

$$MnO_2 + H_2O + e^- \rightarrow MnOOH + OH^- \quad (1)$$

(2) Secondary reaction:

MnOOH was further reduced to $Mn(OH)_2$. Mn_3O_4 is generated during MnOOH discharge and $Mn(OH)_2$ charging. Mn_3O_4 cannot be oxidized or reduced, so it accumulates continuously in the process of charge and discharge, which not only consumes the electrode material, but also increases the internal resistance of the electrode, which directly leads to the attenuation of the discharge capacity of MnO_2 electrode. The reaction formula is:

$$MnOOH + H_2O + e^- \rightarrow Mn(OH)_2 + OH^- \quad (2)$$

In the charge discharge process of MnO_2 electrode, there are both surface adsorption-desorption process and body embedding-desorption process.

1.4.2 Crystal structure of MnO_2

MnO_2 is an octahedral structure, which is a cubic or hexagonal dense packing structure composed of one manganese atom and six coordinated oxygen atoms. The manganese atom is located in the center of the octahedron, the oxygen atom is located at the corner of the octahedron, and the basic structural unit is [MnO_6] (Ghodbane et al., 2008; Jayachandrana et al., 2021).

Due to the different communication modes of MnO_6 octahedrons with different structures, they have different tunnel or interlayer gaps, and the capacitance of manganese dioxide depends on the embedding or de embedding of protons or cations, so only some of them have enough gaps for some ions to be embedded or de embedded in the crystal structure. MnO_2 can be generally divided into three categories. The first category is one-dimensional tunnel structure, including α、β、γ Type; The second type is two-dimensional layered structure, such as δ-MnO_2； The third type is three-dimensional structure, such as λ-MnO_2.

(1) α-MnO_2

The common edges of the basic structural units are arranged along a certain axis in the form of single chain or double chain, and then these single chain or double chain and the adjacent same structure form a body centered tetragonal symmetrical network structure to form [1×2], [2×2] tunnel structure. Cations such as Ba^+, K^+ generally exist in [2×2] tunnels and play a supporting role(Ghodbane et al., 2008).

(2) β-MnO_2

The basic structural unit is formed on the same side [1×1] void tunnel structure. This tunnel structure has a small void cross-sectional area, which is not conducive to ion embedding and embedding. Therefore, if β-MnO_2 is used as battery active material, its discharge polarization is large, and its capacity is lower than that of other manganese oxide crystal forms(Qu et al., 2009).

(3) γ-MnO_2

γ-MnO_2 is formed by the staggered growth of [1×1] and [1×2] tunnels, and the dense hexagonal structure is formed by the staggered growth of single chain and double chain. It is mainly used in zinc manganese battery and lithium manganese battery(De Wolff, 1959).

(4) δ-MnO_2

δ-MnO_2 has a layered structure, which is composed of [MnO_6] octahedral coplanar. This crystal form is characterized by variable cations such as Li^+, K^+, Na^+ and interlayer water. These interlayer ions and interlayer water support the layered structure(Li et al., 2006).

(5) λ-MnO_2

λ-MnO_2 has a typical spinel structure. Oxygen coordination atoms form a square meter stacking structure, and the basic unit is [MnO_6] octahedron. The structure is an interconnected three-dimensional tunnel structure(Li et al., 2021; Du et al., 2021).

1.4.3 Preparation

As a transition metal element, Mn has multiple valence states, and there can be a variety of oxides, such as Mn_3O_4, MnO_2 and MnO. Among them, MnO_2 is widely used in catalysis, energy storage, molecular sieve and adsorption(Brock et al., 1998).

The crystal structure, specific surface area, crystallinity and surrounding micro morphology of MnO_2 prepared by different preparation methods are different. Common methods include sol-gel method, chemical precipitation method, liquid phase redox method, low temperature solid state method, hydrothermal synthesis, and electrodeposition.

The sample prepared by sol-gel method has high purity, but it is affected by drying conditions and is easy to reunite. Chemical precipitation method can directly obtain powder materials with uniform chemical composition and uniform distribution, but it requires high synthesis temperature and is easy to agglomerate. The preparation of electrode powder by low-temperature solid-state method improves the problems of rapid growth and agglomeration of product particles at high temperature, but it has the disadvantages of uneven contact and insufficient reaction. electrodeposition is simple and low cost.

The electrodeposited layer has unique high density and low porosity. By controlling the electrodeposited parameters, the chemical composition, grain size, thickness and other parameters of the deposited film can be accurately controlled. The process is flexible and easy to realize. Electrodeposition methods include constant current/constant voltage method, pulse method and cyclic voltammetry. Different methods will also affect the surface morphology and crystal structure of the deposited layer, and then affect the performance of the capacitor.

Adelkhani et al. prepared MnO_2 electrode by DC and pulse electrodeposition. The results show that the electrode obtained by pulse electrodeposition has larger specific surface area, pore volume and pore diameter, better chemical composition and structure, so it shows better capacitive performance than the electrode obtained by DC electrodeposition(Adelkhani and Ghaemi, 2010).

Sorkhabi et al. electrodeposited nano and amorphous manganese dioxide by constant potential and cyclic voltammetry. Both methods obtained electrodes with good capacitance and high electrochemical stability. However, it was found that the electrode deposited by cyclic voltammetry showed a higher specific capacitance than the electrode deposited by constant potential(Ashassi-Sorkhabi et al., 2014).

1.4.4 Modification

The modification of MnO_2 electrode materials has attracted much attention. Doping and compounding are still common methods for modification. For example, doping a small amount of metal elements into manganese dioxide can improve the conductivity of the electrode, and compounding with some conductive polymers can effectively solve the problem that manganese dioxide is easy to dissolve in the electrolyte due to its unstable structure. The selection of dopant and composite materials, doping and composite methods and the ratio with manganese dioxide are the key to obtain high-quality electrodes. At present, MnO_2 based supercapacitor electrode materials are not only manganese dioxide, but also combine various carbon materials, composites or metals and their oxides to form multi-component composites to make use of the characteristics of each component, which is very helpful to optimize the performance of capacitors.

1.5 Research goal and main contents

Polyaniline (PANI) based supercapacitors have low operating voltage and poor charge discharge reversibility, as PANI is easy to get crushed under high voltage. In this research, MnO_2 is introduced into the supercapacitor (SC) system to modify and strengthen the electrode, aiming to improve the capacitance, operation voltage and reversibility of SC. Quasi-solid is applied to make SC thinner to reduce the loss of electrode active materials and improve the wearability of devices.

2 Experiment

2.1 Materials

The graphite paper (GP) with thickness of 25μm was purchased from Hebei Jingtan Technology Co., Ltd. LiCl was purchased from Xilong Science Co., Ltd. Polyvinyl alcohol (PVA) was purchased from Shanghai Aladdin Biochemical Technology Co., Ltd. The ammonium persulfate (APS) and aniline (ANI) monomers (purity of 99.5%) were purchased from Shanghai Macklin Co., Ltd. Hydrochloric acid (HCl) was purchased from Guangzhou Hewei Pharmaceutical Technology Co., Ltd.

2.2 Supercapacitor preparation

2.2.1 Fabrication of G-PANI paper

Polyaniline was compounded on graphite paper by chemical in-situ polymerization. The graphite paper was 10×10 cm^2 in size.

(1) Use 1 mol / L hydrochloric acid as the environmental solution, the same volume of 0.2 mol / L aniline monomer solution and 0.2 mol / L ammonium persulfate solution was prepared.

(2) Graphite paper was soaked into aniline monomer solution, and then ammonium persulfate solution was added to the above solution at the rate of

2 drops / s at low temperature (0-5 C°). After dropping, continue the reaction for 6 h.

(3) Take out the graphite paper compounded with polyaniline, wash (a large amount of deionized water and an appropriate amount of ethanol and acetone) and dry to obtain flexible paper graphite/polyaniline nanocomposites.

(4) Weigh the dried sample and record.

(5) Repeat (2)-(4) steps for 5 times.

With the increase of load, the surface color of graphite paper becomes darker, the changes of morphology are shown in **Table 1**.

Table 1. Sample changes in morphology and weight during polymerization

Sample photos	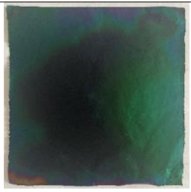				
Polymerization times	1	2	3	4	5
Sample weight（mg）	393	415	444	489	502

The content of polyaniline can be calculated by the weight difference of graphite paper before and after polyaniline compounding. Graphite paper is only served as a conductor, higher mass ratio of PANI improves the effective weight of supercapacitor. The mass of the composite increases from 361 mg to 502 mg. The mass ratio of PANI reaches to 39%, as shown in **Figure. 5**.

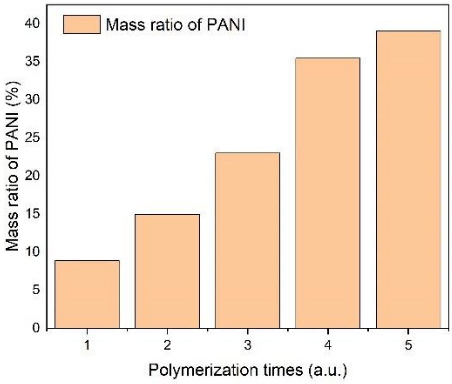

Figure. 5 Mass ratio of PANI

2.2.2 Loading MnO_2 on the surface of G-PANI

In this research, electrodeposition was introduced to load MnO_2 on the surface of G-PANI. The experimental steps are as follows:

(1) Cut the loaded G-PANI paper into pieces of 1×3 cm^2.

(2) Make the sample (G-PANI) as the positive electrode, the platinum electrode as the negative electrode. Electrodeposit in 1M $(CH_3COO)_2Mn$ solution, under 10 mA constant current for 30 minutes. Only 1×1cm^2 was immersed in the electrolyte.

(3) Wash, dry and weigh.

The sample loaded with MnO_2 is marked as G-PANI-MnO_2.

2.2.3 Preparation of quasi solid electrolyte

In previous attempts, MnO_2 was found to diffuse easily into the electrolyte. In this experiment, polyvinyl alcohol (PVA) was added into the electrolyte to delay the diffusion process. First, prepare 3M LiCl aqueous solution as usual; then add 20% Polyvinyl alcohol (PVA) by weight of solution, heat and stir to form quasi-solid electrolyte.

2.2.4 Supercapacitor assembly

Asymmetric supercapacitor (aSC):

Make G-PANI-MnO_2 as positive electrode and G-PANI as negative electrode.

Smear gel electrolyte on the $1\times1cm^2$ part of G-PANI-MnO_2, which was loaded with MnO_2. smear the negative electrode on the same site. The two sides with electrolyte were superimposed on each other and keep 1-2mm between the electrodes. Seal with adhesive tape, apply silver glue on the end and stick strip platinum.

Symmetric supercapacitor (control group):

Make two pieces of G-PANI paper as positive and negative electrodes, respectively. The assembly method is the same as above.

The SCs assembled are shown on **Figure 6**.

Figure. 5 SCs assembled

2.3 Materials characterization

2.3.1 Scanning electron microscope

The microstructure images were taken by a field emission scanning electron microscope (SEM, Hitachi SU8010).

2.3.2 X-ray diffraction

The X-ray diffraction (XRD) test was conducted by an X-ray diffractometer (Rigaku Ultima IV) with Cu Kα radiation (λ = 0.15405 nm).

2.3.3 X-ray photoelectron spectroscopy

X-ray photoelectron spectroscopy (XPS) was conducted on a Thermo ScientificTM K-AlphaTM+ spectrometer equipped with a monochromatic Al Kα X-ray source (1486.6 eV) operating at 100 W.

The sample was analyzed under vacuum (P < 10−8 mbar) with a pass energy of 150 eV (survey scans) or 50eV (high-resolution scans).

All peaks would be calibrated with C1s peak binding energy at 284.8 eV for adventitious carbon.

2.4 Electrochemical properties measurements

2.4.1 Rate performance

The rate test was performed using a battery testing system (Wuhan LAND, CT3001A).

2.4.1.1 Single electrode rate performance

Three-electrode system was introduced. Make sample as working electrode, Ag/AgCl as reference electrode, platinum electrode as counter electrode.

For aSC, set the current at 1/2/3/4mA, respectively, with an operation window of 2.0V. For sSC, set the current at 1/2/3/4 mA, with an operation window of 1.0V.

2.4.1.2 Supercapacitor rate performance

For aSC, set the current at 1/2/3/4mA, respectively, with an operation window of 2.0V. For sSC, set the current at 1/2/3/4 mA, with an operation window of 1.0V.

2.4.2 Cycle life performance

The cycle life measurement was performed with a battery testing system (Wuhan LAND, CT3001A).

For aSC, constant current was set at 2mA with an operation window of 2.0V. For sSC, constant current was set at 2mA with an operation window of 1.0V.

3 Simulation

3.1 Background

In previous work, MnO_2 was found to continuously diffuse into the electrolyte during charge/discharge process. After several design improvements, inhibiting the loss of MnO_2 is still not satisfactory. A model was built up to simulate the process of diffusion.

3.2 Modelling

A two-dimensional lattice of 100×100 sites was employed throughout the simulation. Each site represents a small part of electrolyte between two electrodes. The left border represented the G-PANI-MnO_2 electrode, while the right represented the G-PANI electrode. At the beginning of charge and discharge, MnO_2 focused on the left border, the interface between G-PANI-MnO_2 electrode and electrolyte, exactly. There is no MnO_2 in the electrolyte or the right border, as shown in **Figure. 7**.

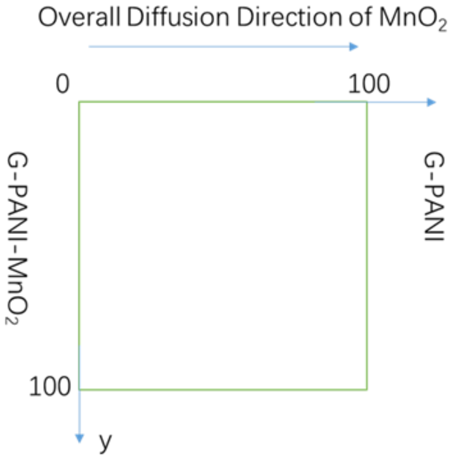

Figure. 6 Schematic diagram of MnO_2 diffusion during charging and discharging

The concentration of MnO_2 at site i (coordinate number (x, y)) is represented by P_i, which can be governed by the first-order rate equation:

$$\frac{dP_i}{dt} = \sum_j (P_j W_{ji} - P_i W_{ij})$$

On the left border, when x=0, the initial MnO_2 concentration P[0, y] = 1.0

The W (x, y, d) value will be updated as the diffusion proceeds. In this case, all W values were fixed at 1 throughout the entire process.

P updates automatically with diffusion.

4 Results and Discussion

4.1 Synthesis of electrode

In this study, PANI in the GP based composites was used to induce MnO_2. The graphite paper was first polymerized with PANI and cut into the designed pattern. Then the specific part of the electrode was electrodeposited to introduce MnO_2 onto the G-PANI framework, boosting the electron transfer between the outer capacitive MnO_2 and the inner conductive GP. This synthesis method provides several benefits for the highly efficient utilization of MnO_2. First, MnO_2 is directly coated on a conductive framework forming a flexible and freestanding electrode, without being mixed with other agents and pasted on a current collector as powdery MnO_2 usually did. Second, the growth of MnO_2 on the conductive template is spatially controlled, thus making the electrode highly designable.

4.1.1 Formation of PANI

Polyaniline (PANI) prepared in HCl solution was dark green. the polymerization of aniline in acidic solution is through the coupling between N atom and C atom at C-4 position of aromatic ring, to form molecular long chain. This kind of PANI has high conductivity, electrochemical activity, and stability.

Polymerization at low temperature (ice water bath) is conducive to increase the molecular weight of PANI and obtain products with narrow molecular weight distribution.

4.1.2 Form changes of MnO_2

During the charging process, the electrolyte cations enter the MnO_2 bulk phase through the electrode surface to complete the embedding and realize the charge storage. During the discharge process, the cation is separated from the MnO_2 bulk phase to complete the charge release. In this process, valence change of Mn^{4+}/Mn^{3+} only occurs on the surface of electrode. MnO_2 is finally dissolved into the electrolyte in molecular state.

4.2 Scanning electron microscope

According to the design, the immersed part will be loaded with MnO_2 while the other part remains unchanged. This was verified in **Figure. 8** that a fuzzy boundary can be found as indicated by the dashline. The brighter part in the image corresponds to the MnO_2 due to its lower electric conductivity.

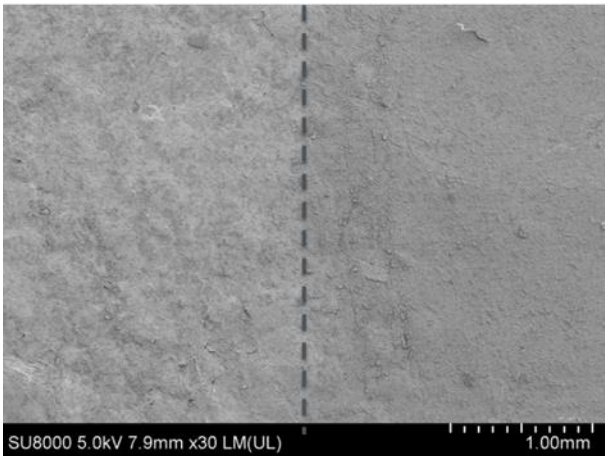

Figure. 7 SEM images of the elctrode among the boundary between G-PANI-MnO_2 and G-PANI

Compared to the original G-PANI composites (**Figure. 9**(a)), the surface of the electrode became much rougher after the treatment with nano size particles coated around GP (**Figure. 9**(a)).

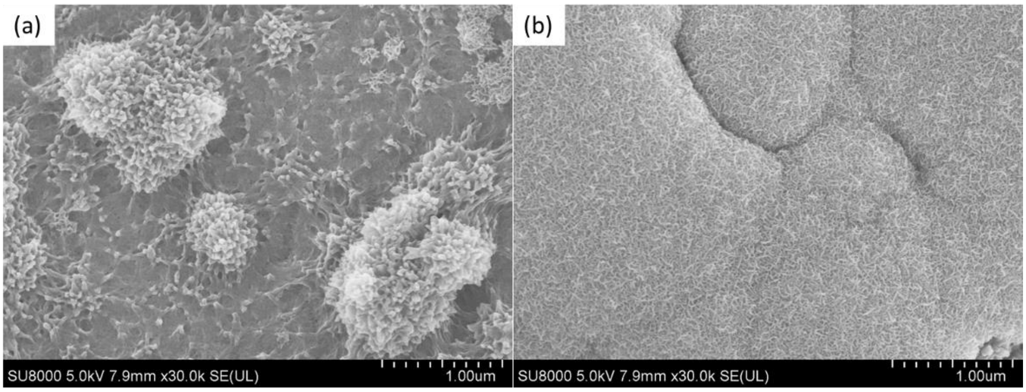

Figure. 8 High magnification SEM images of (a) G-PANI and (b) G-PANI-MnO_2

4.3 X-ray diffraction (XRD) Measurement of G-PANI-MnO_2 and G-PANI

As shown in **Figure. 10**, XRD images are almost indistinguishable before and after electrodeposition. The peaks in the image are typical peaks of graphene with orientation of (002), which means no MnO_2 was detected. It may be for two reasons: the content of MnO_2 is less; MnO_2 on the surface is amorphous.

Amorphism refers to the structure of some incompletely crystalline amorphous regions (amorphous regions) or the composition of some amorphous solids (amorphous). Amorphous regions are composed of molecules that fail to crystallize due to complex conformation, molecules that are excluded from microcrystals due to differences in molecular weight, and bound molecules. The arrangement of atoms or molecules in it has no periodicity, so there is no diffraction peak.

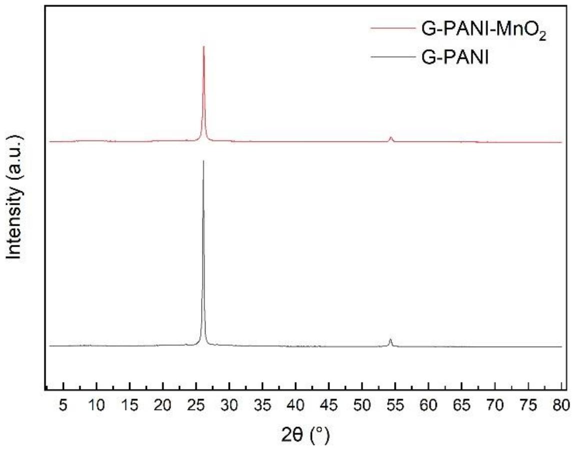

Figure. 9 XRD image of G-PANI-MnO_2 and G-PANI with typical peaks of graphene(002)

4.4 X-ray photoelectron spectroscopy

The characteristic spin-energy separation of 11.70 eV between Mn $2P_{1/2}$ (653.88 eV) and Mn $2P_{3/2}$ (642.18 eV) peaks is consistent with the previous reported MnO_2, as shown in **Figure. 11**. In comparison, no peak was observed in the G-PANI composites in this range. XPS Verified the existence of Mn.

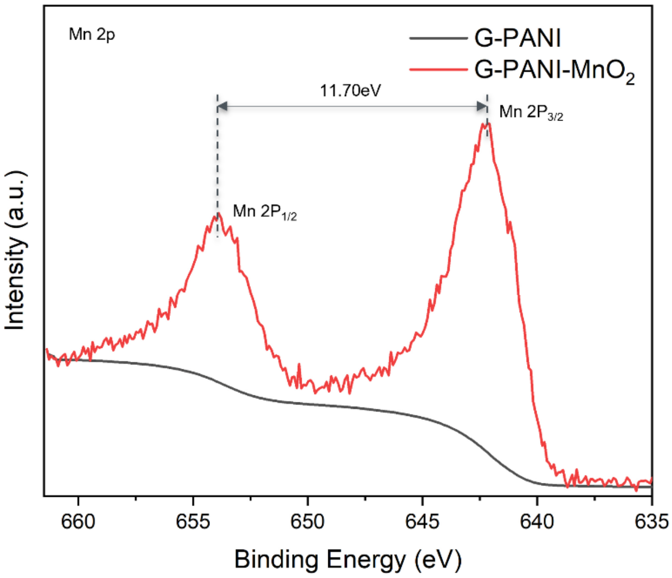

Figure. 10 XPS spectra of G-PANI-MnO_2 and G-PANI

4.5 Electrochemical Characterizations

4.5.1 Rate performance

The G-PANI-MnO_2 electrode showed quite symmetric GCD curves (**Figure 12**(a)) and demonstrates a good reversibility of the charging-discharging process.

Although PANI has been widely adopted as positive electrode of SC, its potential window is limited that it’s usually no higher than 0.8 V. Under 1V, the structure of PANI was destroyed and the reversibility of the redox reaction was poor. With MnO_2 deposited, extra pseudocapacitance was provided and it kept more stable under the same voltage. The results showed that G-PANI electrode not only shows a limited capacitance, but also poor reversibility as proved by the GCD test (**Figure. 12**(b)).

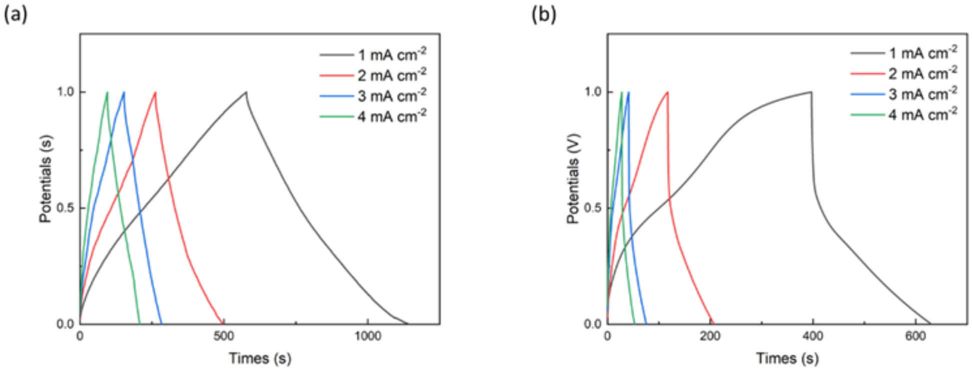

Figure. 11 GCD curves of G-PANI-MnO_2 (a) and G-PANI(b) electrodes under different current densities (potentials vs Ag/AgCl)

Compared with sSC, as shown in **Figure. 13**, aSC had longer charge discharge cycle, which showed better capacitance. But with the expansion of operation window (from 1.0V to 2.0V), the symmetry of GCD curve decreases, the reversibility is poorer., MnO_2 began to melt under higher voltage, which made the reversibility of reaction drop.

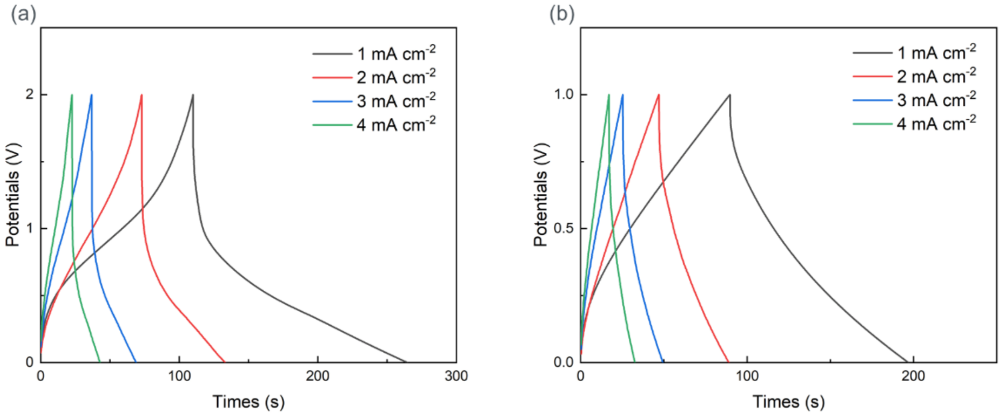

Figure. 12 GCD curves of (a)aSC and (b)sSC under 1/2/3/4 mA.

4.5.2 Cycle life performance

As shown in **Figure. 14**(a), in the first 40 cycles, the capacitance of aSC increased from 170.5 mF/cm^2 to 178.2mF/cm^2, which may undergo electrode activation process.

When the reaction time is short, the capacitance is basically provided by PANI, and MnO_2 does not bring much help to improve the pseudocapacitance; In addition, MnO_2 reduces the attachment sites on the PANI surface, making it difficult for electrolyte ions to be embedded and detached quickly.

In the first 1000 cycles, the discharge capacitance of new supercapacitor is 30% higher than that was composed of symmetrical polyaniline electrode overall. After 1000 cycles of charge and discharge, the capacitance decreases by only 10%.

In this process, compared with sSC, MnO_2 on the surface of G-PANI provided extra capacitance. On the one hand, it provided additional ion adsorption and desorption sites; On the other hand, it provided pseudocapacitance through rapid and reversible redox reaction.

But when the cycle number reached 5000 times, as shown in **Figure. 14**(b), the discharge capacitance of aSC dropped faster than that of sSC.

Under continuous relatively high operation window, MnO_2 on the surface of PANI start melting and constantly diffuses into the electrolyte. In addition, some PANI peeled off from the surface of graphite paper during electroplating, which reduced the initial capacitance. In long period, the improvement measures can only delay but cannot stop the diffusion process.

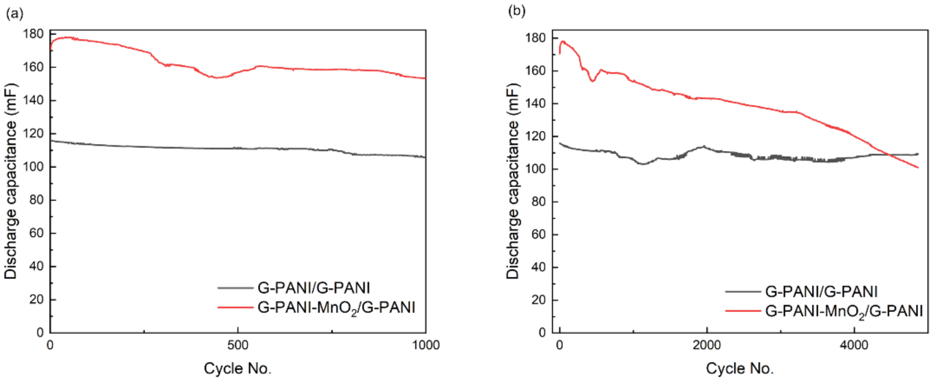

Figure. 13 Cycle life test of aSC and sSC. (a) 1000 cycles; (b) 5000cycles.

4.6 Simulation of MnO_2 diffusion

With the charge discharge process, MnO_2 begins to diffuse to the other side, which is governed by the first-order rate equation.

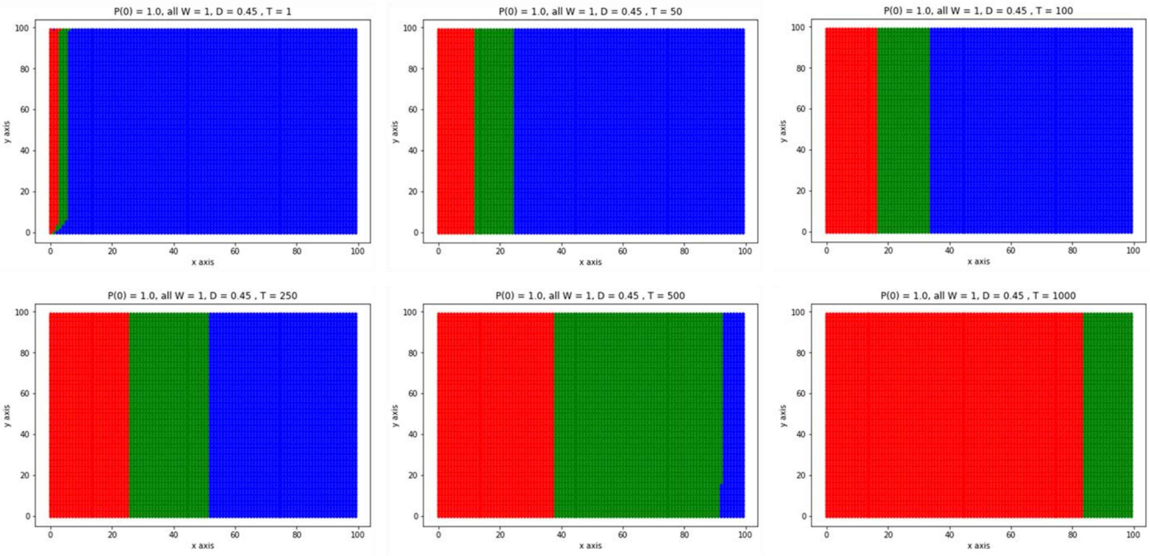

Figure. 14 Concentration distribution of MnO_2 when T=1,50,100,250,500,1000. Red: $0.6<P\leq 1$; Green: $0.3<P\leq 0.6$; Blue: $0\leq P\leq 0.3$(P: concentration of MnO_2).

Figure. 15 shows MnO_2 concentration distribution at different times. This is an ideal simulation. The device may not be absolutely sealed, which means water may evaporate from the top and the bottom border. The closer to the boundary, the greater the evaporation. The evaporation varies longitudinally, which means the diffusion coefficient varies near the border. The diffusion coefficient of a site is related to the reaction time and the distance from the border. This situation may need to be considered.

5 Conclusion

In conclusion, the introduction of MnO_2 provided extra ion adsorption and desorption sites and redox pseudocapacitance, which effectively improve the capacitance of supercapacitors. MnO_2 formed a certain protection for PANI, slowed down the crushing of PANI, improved the operation voltage and reversibility of SC. In short period, aSC introduced with MnO_2 showed better capacitance than sSC. Even with higher operation window, the capacitance can still be 30% higher than that of sSC.

In long period, although quasi-solid electrolytes slowed down the diffusion, MnO_2 inevitably diffused into the electrolyte. The loss of electrode active material reduced the capacitance of SC. A model was built up to reflect the process of diffusion.

6 Reference

Simon P., Gogotsi Y., 2009. Materials for electrochemical capacitors. Nat. Mater. https://doi.org/10.1038/nmat2297

Conway B.E., 1999. Electrochemical supercapacitors: scientific fundamentals and technological applications. New York: Plenum Press.

Gibney E.,2015. The inside story on wearable electronics. Nature, 528(7580): 26-28. https://doi.org/10.1038/528026a

Kenry, Yeo J.C., Lim C.T., 2016. Emerging flexible and wearable physical sensing platforms for healthcare and biomedical applications. Microsystems & nanoengineering, 2(1): 16043. https://doi.org/10.1038/micronano.2016.43

Kim J., Campbell A.S, de ávila B.E., Wang J., 2019. Wearable biosensors for healthcare monitoring. Nat. Biotechnol., 37(4): 389-406. https://doi.org/10.1038/s41587-019-0045-y

Yu X., Xie Z., Yu Y., Lee J., Vazquez-Guardado A., Luan H., Ruban J., Ning X., Akhtar A., Li D., Ji B., Liu Y., Sun R., Cao J., Huo Q., Zhong Y., Lee C., Kim S., Gutruf P., Zhang C., Xue Y., Guo Q., Chempakasseril A., Tian P., Lu W., Jeong J., Yu Y., Cornman J., Tan C., Kim B., Lee K., Feng X., Huang Y., Rogers J.A.,2019. Skin-integrated wireless haptic interfaces for virtual and augmented reality. Nature, 575(7783): 473-479. https://doi.org/10.1038/s41586-019-1687-0

Hu H., Pei Z., Ye C., 2015. Recent advances in designing and fabrication of planar micro-supercapacitors for on-chip energy storage. Energy Storage Mater., 1: 82-102. https://doi.org/10.1016/j.ensm.2015.08.005

Hou R., Gund G.S, Qi K., Nakhanivej P., Liu H.F., Li F., Xia B.Y., Park H.S., 2019. Hybridization design of materials and devices for flexible electrochemical energy storage. Energy Storage Mater., 19: 212-241. https://doi.org/10.1016/j.ensm.2019.03.002

Jost K., Dion G., Gogotsi Y., 2014. Textile energy storage in perspective. J. Mater. Chem. A, 2(28): 10776. https://doi.org/10.1039/C4TA00203B

Zhang L.L., Zhao X.S., 2009. Carbon-based materials as supercapacitor electrodes. Chem. Soc. Rev., 38(9): 2520. https://doi.org/10.1039/b813846j

Pan L.J., Qiu H., Dou C.M., Li Y., Pu L., Xu J.B., Shi Y., 2010. Conducting polymer nanostructures: template synthesis and applications in energy storage. INTERNATIONAL JOURNAL OF MOLECULAR SCIENCES, 11(7): 2636-2657 https://doi.org/10.3390/ijms11072636

Winter M., Brodd R.J., 2004. What Are Batteries, Fuel Cells, and Supercapacitors? Chem. Rev., 104(10): 4245-4270. https://doi.org/10.1021/cr020730k

Sun G., Yang H., Zhang G., Qu L.T., 2018. A capacity recoverable zinc-ion micro-supercapacitor. Energ. Environ. Sci., 11(12): 3367-3374. https://doi.org/10.1039/C8EE02567C

Shirakawa H., Louis E.J., Macdiarmid A.G., Chiang C.K., Heeger A.J., 1977. Synthesis of Electrically Conducting Organic Polymers: Halogen Derivatives of Polyacetylene. J. Chem. Soc. Chem. Commun., 16, 578. http://dx.doi.org/10.1039/c39770000578

Nigrey P.J., Macdiarmid A.G., Heeger A.J., 1979. J. Chem. Soc. Chem. Commun., 594. https://doi.org/10.1039/C39790000594

Eftekhari A., Jafarkhani P., 2014. Galvanodynamic synthesis of polyaniline: A flexible method for the deposition of electroactive materials. Journal of Electroanalytical Chemistry. https://doi.org/10.1016/j.jelechem.2014.01.018

Bian L.J., Luan F., Liu S.S., Liu X.X., 2012. Self-doped polyaniline on functionalized carbon cloth as electroactive materials for supercapacitor. Electrochimica Acta. https://doi.org/10.1016/j.electacta.2011.12.012

Tanguy N.R., Thompson M., Yan N., 2018. A review on advances in application of polyaniline for ammonia detection. Sensors and Actuators B: Chemical. https://doi.org/10.1016/j.snb.2017.11.008

RudgeA., Raistrick I., Gottesfeld S., Ferraris J.P., 1994. A study of the electrochemical properties of conducting polymers for application in electrochemical capacitors. Electrochim. Acta. https://doi.org/10.1016/0013-4686(94)80063-4

Arbizzani C., Mastragostino M., Meneghello L., 1996. Polymer-based redox supercapacitors: a comparative study. Electrochim. Acta. https://doi.org/10.1016/0013-4686(95)00289-Q

Mastragostino M., Arbizzani C., Meneghello L., Paraventi R., 1996. Electronically conducting polymers and activated carbon: electrode materials in supercapacitor technology. Adv. Mater. https://doi.org/10.1002/adma.19960080409

Hu C., Chu C., 2001. Electrochemical impedance characterization of polyaniline-coated graphite electrodes for electrochemical capacitors — effects of film coverage/thickness and anions. J. Electroanal. Chem. https://doi.org/10.1016/S0022-0728(01)00385-0

Macdiarmid A.G., Chiang J.C., Richter A.F., Epestin A.J., 1987. Polyaniline - a new concept in conducting polymers. Synthetic Met., 18(1-3): 285-290 https://doi.org/10.1016/0379-6779(87)90893-9

Wu W., Pan D., Li Y., Zhao G., Jing L., Chen S., 2015. Facile fabrication of polyaniline nanotubes using the self-assembly behavior based on the hydrogen bonding: a mechanistic study and application in high-performance electrochemical supercapacitor electrode. Electrochim. Acta. https://doi.org/10.1016/j.electacta.2014.11.130

Gawli Y., Banerjee A., Dhakras D., Deo M., Bulani D., Wadgaonkar P., Shelke M., Ogale S., 2016. 3D polyaniline architecture by concurrent inorganic and organic acid doping for superior and robust high rate supercapacitor performance. Sci. Rep. https://doi.org/10.1038/srep21002

Patil D.S., Shaikh J.S., Dalavi D.S., Karanjkar M.M., Devan R.S., Ma Y.R., Patil P.S., 2011. An Mn doped polyaniline electrode for electrochemical supercapacitor. J. Electrochem. Soc. https://doi.org/10.1149/1.3561428

Giri S., Ghosh D., Das C.K., 2013. In situ synthesis of cobalt doped polyaniline modified graphene composites for high performance supercapacitor electrode materials. J. Electroanal. Chem. https://doi.org/10.1016/j.jelechem.2013.01.038

Zhang H., Zhao Q., Zhou S., Liu N., Wang X., Li J., Wang F., 2011. Aqueous dispersed conducting polyaniline nanofibers: promising high specific capacity electrode materials for supercapacitor. J. Power Sources. https://doi.org/10.1016/j.jpowsour.2011.08.066

Fan L., Hu Y., Maier J., Adelhelm P., Smarsly B., Antonietti M., 2007. High electroactivity of polyaniline in supercapacitors by using a hierarchically porous carbon monolith as a support. Adv. Funct. Mater. https://doi.org/10.1002/adfm.200700518

Cho S., Shin K., Jang J., 2013. Enhanced electrochemical performance of highly porous supercapacitor electrodes based on solution processed polyaniline thin films. ACS Appl. Mater. Interfaces. https://doi.org/10.1021/am402702y

Chen W., Rakhi R.B., Alshareef H.N., 2013. Facile synthesis of polyaniline nanotubes using reactive oxide templates for high energy density pseudocapacitors. J. Mater. Chem. A. https://doi.org/10.1039/c3ta00499f

Zhou Q., Li C.M., Li J., Lu J., 2008. Electrocatalysis of template-electrosynthesized Cobalt−Porphyrin/polyaniline nanocomposite for oxygen reduction. J. Phys. Chem. C. https://doi.org/10.1021/jp8077375

Zhang D.Z., Wang Y.Y., 2006. Synthesis and applications of one-dimensional nano-structured polyaniline: an overview. Mat. Sci. Eng. B-Solid, 134(1): 9-19 https://doi.org/10.1016/j.mseb.2006.07.037

Ma L.X., Wang C.S., Yang W.M.,2009. Synthesis of Conducting Polyaniline Using Compound Oxidant. Advanced Materials Research. https://doi.org/10.4028/www.scientific.net/AMR.87-88.300

Ayad M.M., Shenashin M.A., 2004. Polyaniline film deposition from the oxidative polymerization of aninie using $K_2Cr_2O_7$. European Polymer Journal. https://doi.org/10.1016/j.eurpolymj.2003.09.002

Hirase R., Shikata T., Shirai M., 2014. Selective formation of polyaniline on wool by chemical polymerization, using potassium iodate. Synthetic Metals. https://doi.org/10.1016/j.synthmet.2004.06.009

Gosk J., Kulszewicz-Bajer I., Twardowski A., 2016. Magnetic properties of polyaniline doped with $FeCl_3$. Synthetic Metals. https://doi.org/10.1016/j.synthmet.2006.02.003

Sarma T.K., Chowdhury D., Paula A., Chattopadhyay A., 2002. Synthesis of Au nanoparticle–conductive polyaniline composite using H_2O_2 as oxidising as well as reducing agent. Chemical Communications. https://doi.org/10.1039/B201014C

Elkais A., Milica G., Jugović B., Stevanović J., Nikolić N., Grgur B.,2011. Electrochemical synthesis and characterization of polyaniline thin film and polyaniline powder. Progress in Organic Coatings. https://doi.org/10.1016/j.porgcoat.2010.12.004

Mezgebe M.M., Xu K.B., Wei G., Guang S.Y., Xu H.Y., 2019. Polyaniline wrapped manganese dioxide nanorods: Facile synthesis and as an electrode material for supercapacitors with remarkable electrochemical properties. Journal of Alloys and Compounds. https://doi.org/10.1016/j.jallcom.2019.04.295

Ram M.S., Palaniappan P.S., 2003. Benzoyl peroxide oxidation route to polyaniline salt and its use as catalyst in the esterification reaction. Molecular Catalysis. https://doi.org/10.1016/S1381-1169(03)00157-2

Xie P., Rong M.Z., Zhang M.Q., 2016. Moisture battery formed by direct contact of magnesium with foamed polyaniline. Angew. Chem. Int. Ed. https://doi.org/10.1002/anie.201510686

Pham-Cong D., Park J.S., Kim J.H., Kim J., Braun P.V., Choi J.H., Kim S.J., Jeong S.Y., Cho C.R., 2017. Enhanced cycle stability of polypyrrole-derived nitrogen-doped carbon-coated tin oxide hollow nanofibers for lithium battery anodes. Carbon. https://doi.org/10.1016/j.carbon.2016.09.057

Alguail A.A., Al-Eggiely A.H., Gvozdenović M.M., Jugović B.Z., Grgur B.N., 2016. Battery type hybrid supercapacitor based on polypyrrole and lead-lead sulfate. J. Power Sources. https://doi.org/10.1016/j.jpowsour.2016.02.081

Vega-Rios A., Rentería-Baltiérrez F.Y., Hernández-Escobar C.A., Zaragoza-Contreras E.A., 2013. A new route toward graphene nanosheet/polyaniline composites using a reactive surfactant as polyaniline precursor. Synth. Met. https://doi.org/10.1016/j.synthmet.2013.09.014

Jayakumar A., Yoon Y., Wang R., Lee J.,2015. Novel graphene/polyaniline/MnOx 3D-hydrogels obtained by controlled morphology of MnOx in the graphene/polyaniline matrix for high performance binder-free supercapacitor electrodes. RSC Adv. https://doi.org/10.1039/c5ra16884h

Yu T., Zhu P., Xiong Y., Chen H., Kang S., Luo H., Guan S., 2016. Synthesis of microspherical polyaniline/graphene composites and their application in supercapacitors. Electrochim. Acta. https://doi.org/10.1016/j.electacta.2016.11.033

Wang L., Wu T., Du S., Pei M., Guo W., Wei S., 2016. High performance supercapacitors based on ternary graphene/Au/polyaniline (PANI) hierarchical nanocomposites. RSC Adv. https://doi.org/10.1039/c5ra23549a

Miao F., Shao C., Li X., Wang K., Liu Y., 2016. Flexible solid-state supercapacitors based on freestanding nitrogen-doped porous carbon nanofibers derived from electrospun Polyacrylonitrile@polyaniline nanofibers. J. Mater. Chem. A. https://doi.org/10.1039/c6ta00015k

Imani A., Farzi G., 2015. Facile route for multi-walled carbon nanotube coating with polyaniline: tubular morphology nanocomposites for supercapacitor applications. J. Mater. Sci. Mater. Electron. https://doi.org/10.1007/s10854-015-3377-5

Uppugalla S., Male U., Srinivasan P., 2014. Design and synthesis of heteroatoms doped carbon/polyaniline hybrid material for high performance electrode in supercapacitor application. Electrochim. Acta. https://doi.org/10.1016/j.electacta.2014.09.047

Dhibar S., Bhattacharya P., Hatui G., Sahoo S., Das C.K., 2014. Transition metal-doped polyaniline/single-walled carbon nanotubes nanocomposites: efficient electrode material for high performance supercapacitors. ACS Sustain. Chem. Eng. https://doi.org/10.1021/sc5000072

Xiang X., Zhang W., Yang Z., Zhang Y., Zhang H., Zhang H., Guo H., Zhang X., Li Q., 2016. Smart and flexible supercapacitor based on a porous carbon nanotube film and polyaniline hydrogel. RSC Adv. https://doi.org/10.1039/c6ra00705h

Zhou Y.F., Wang Q.J., Wu J.B., Wu R.R., Huang Y.F., Ye Y., Qin H.W., Zhang P.P., 2018. A Novel All-Solid-State Ion-Selective Electrode with Selenite-doped Polyaniline. Int. J. Electrochem. Sci., 13: 12140-12154 https://doi.org/10.20964/2018.12.610

Lu W.K., Elsenbaumer R.L., Wessling B., 1995. Corrosion protection of mild-steel by coatings containing polyaniline. Synthetic Met., 71(1-3): 2163-2166 https://doi.org/10.1016/0379-6779(94)03204-J

Bhandari H, Choudhary V, Dhawan S.K., 2009. Synergistic effect of copolymers composition on the electrochemical, thermal, and electrical behavior of 5-lithiosulphoisophthalic acid doped poly(aniline-co-2-isopropylaniline):

synthesis, characterization, and applications. Polym. Advan. Technol., 20(12): 1024-1034 https://doi.org/10.1002/pat.1359

Sairam M., Nataraj S.K., Aminabhavi T.M., Sukumar R., Madhusoodana C.D., 2006. Polyaniline Membranes for Separation and Purification of Gases, Liquids, and Electrolyte Solutions. Separation & Purification Reviews, 35(4):249 https://doi.org/10.1080/15422110600859727

Kobayashi T., Yoneyama H., Tamura H., 1984. Electrochemical reactions concerned with electrochromism of polyaniline film-coated electrodes. J. Electroanal. Chem., 177(1-2): 281-291 https://doi.org/10.1016/0022-0728(84)80229-6

Burroughes J.H., Bradley D.D.C., Brown A.R., Marks, R.N., Mackay K., Friend R.H., Burn P.L., Holmes A.B., 1990. Light-emitting-diodes based on conjugated polymers. Nature, 347(6293): 539-541 https://doi.org/10.1038/347539a0

He X.J., Li X.J., Wang X.T., Zhao N., Yu M.X., Wu M.B., 2015. Efficient preparation of porous carbons from coal tar pitch for high performance supercapacitors. New Carbon Materials, 29(6):493-502 https://doi.org/10.1016/S1872-5805(14)60150-5

Li L., Tan L., Li G.N., Zhang Y.M., Wu B.H., 2017. Insight into synergy within multi-decorated graphene 3D networks for high performance supercapacitor. Journal of Solid State Chemistry, 251:266-273 https://doi.org/10.1016/j.jssc.2017.05.002

Güven Özdemir Z., Yilmaz Canli N., Senkal B.F., Gürsel Y., Okutan M., 2015. Super-capacitive behavior of carbon nano tube doped 11-(4-cyanobiphenyl-4-oxy) undecan-1-ol. Journal of Molecular Liquids, 211: 442-447 https://doi.org/10.1016/j.molliq.2015.07.026

Sun H., She P., Xu K.L., Shang Y.X., Yin S.Y., Liu Z.Y., 2015. A self-standing nanocomposite foam of polyaniline@reduced graphene oxide for flexible super-capacitors. Synthetic Metals, 209: 68-73 https://doi.org/10.1016/j.synthmet.2015.07.001

Bahloul A., Nessark B., Briot E., Groult H., Mauger A., Zaghib K., Julian C.M., 2013. Polypyrrole-covered MnO_2 as electrode material for supercapacitor. Journal of Power Sources, 240: 267-272 https://doi.org/10.1016/j.jpowsour.2013.04.013

Wang P.F., Liu H., Xu Y.X. Chen Y.F. Yang J., Tan Q.Q., 2016. Supported ultrafine ruthenium oxides with specific capacitance up to 1099 F g^{-1} for a supercapacitor. Electrochimica Acta, 240: 267-272 https://doi.org/10.1016/j.jpowsour.2013.04.013

Yang M.H., Hong S.K., Choi. B.G., 2015. Hierarchical MnO_2 nanosheet arrays on carbon fiber for high-performance pseudocapacitors. Journal of

Electroanalytical Chemistry, 759(2): 95-100 https://doi.org/10.1016/j.jelechem.2015.10.038

Yu W., Li B.Q., Ding S.J., 2016. Electroless fabrication and supercapacitor performance of CNT@NiO-nanosheet composite nanotubes. Nanotechnology, 27(7): 075605 https://doi.org/10.1088/0957-4484/27/7/075605

Liu K.C., Anderson M.A., 1996. Porous Nickel Oxide Films for Electrochemical Capacitors. Journal of The Electrochemical Society. https://doi.org/10.1557/PROC-393-427

Lin C., Ritter J.A., Popov B.N., 1998. Characterization of Sol-Gel-Derived Cobalt Oxide Xerogels as Electrochemical Capacitors. Journal of The Electrochemical Society, 145(12): 4097-4103 https://doi.org/10.1149/1.1838920

Brock S., Duan N.G., Tian Z., Giraldo O., Zhou H., Suib S., 1998. A Review of Porous Manganese Oxide Materials. Chemistry of Materials. https://doi.org/10.1021/CM980227H

Ghodbane O., Pascal J.L., Favier F., 2008. Microstructural effects on Charge Storage Properties in MnO2 based Electrochemical Supercapacitors. The Electrochemical Society, 16: 235. https://doi.org/10.1149/1.2985649

Jayachandrana M., Rose A., Maiyalagan T., Poongodic N., Vijayakumar T., 2021. Effect of various aqueous electrolytes on the electrochemical performance of α-MnO_2 nanorods as electrode materials for supercapacitor application. Electrochimica Acta. https://doi.org/10.1016/j.electacta.2020.137412

Qu Q.T., Zhang P., Wang B., Chen Y.H., 2009. Electrochemical Performance of MnO_2 Nanorods in Neutral Aqueous Electrolytes as a Cathode for Asymmetric Supercapacitors. The Journal of Physical Chemistry C. https://doi.org/10.1021/jp8113094

De Wolff P.M., 1959. Interpretation of some γ-MnO_2 diffraction patterns. Acta Crystallographica. https://doi.org/10.1107/S0365110X59001001

Li W.N., Yuan J., Shen X.F., Gomez-Mower S., Xu L.P., SithambaramS., Aindow M., Suib S.L., 2006. Hydrothermal Synthesis of Structure- and Shape-Controlled Manganese Oxide Octahedral Molecular Sieve Nanomaterials. Advanced Functional Materials. https://doi.org/10.1002/adfm.200500504

Li L., YangQ.L., WangD., Peng Y., Yan J.L., Li J.H., Crittenden J., 2021. Facile synthesis λ-MnO_2 spinel for highly effective catalytic oxidation of benzene. Chemical Engineering Journal. https://doi.org/10.1016/j.cej.2020.127828

Du X., Guan G.Q., Li X.M., Jagadale A.D., Ma X.L., Wang Z.D., Hao X.G., Abudulac A., 2021. A novel electroactive λ-MnO2/PPy/PSS core–shell nanorod coated electrode for selective recovery of lithium ions at low concentration. Journal of Materials Chemistry A. https://doi.org/10.1039/C6TA05985F

Jaidev, Jafri R.I., Mishra A.K., 2011. Polyaniline-MnO_2 nanotube hybrid nanocomposite as supercapacitor electrode material in acidic electrolyte. Journal of Materials Chemistry. https://doi.org/10.1039/C1JM13191E

Adelkhania H.,Ghaemi M., 2010. Characterization of manganese dioxide electrodeposited by pulse and direct current for electrochemical capacitor. Journal of Alloys and Compounds. https://doi.org/10.1016/j.jallcom.2009.12.042

Ashassi-Sorkhabi H., Asghari E., La’le Badakhshan P., 2014. Potentiostatic and cyclic voltammetric deposition of nanostructured manganese oxide for supercapacitor applications. Current Applied Physics. https://doi.org/10.1016/j.cap.2013.11.001